論文 / 著書情報
Article / Book Information

論題(和文)	Study on particle reduction method of model under wind response
Title(English)	Study on particle reduction method of model under wind response
著者(和文)	Yizhou LONG, 佐藤大樹, 陳引力, 田中英之, 曽根孝行, 今野大輔, 渡井一樹
Authors(English)	Yizhou Long, Daiki Sato, Yinli Chen, Hideyuki Tanaka, Takayuki Sone, Daisuke Konno, Kazuki Watai
出典 / Citation	日本建築学会関東支部研究報告集, Ⅰ, , pp. 449-452
Citation(English)	, Ⅰ, , pp. 449-452
発行日 / Pub. date	2025, 3
権利情報	一般社団法人 日本建築学会

2024年度日本建築学会
関東支部研究報告集Ⅰ
2025年3月

Study on particle reduction method of model under wind response

構造ー振動

High rise building, Stiffness damper, Wind response
Particle reduction method, CFD

正会員 ○ Yizhou LONG[*1] 正会員 Daiki SATO[*1]
Yinli CHEN[*1] Hideyuki TANAKA[*2]
Takayuki SONE[*2] Daisuke KONNO[*2]
Kazuki WATAI[*2]

1. Introduction

In the study of wind-resistant design for high-rise buildings, understanding the structural dynamic characteristics and wind-induced responses is crucial. Analyzing the full-scale detailed models of high-rise structures is time-consuming. To address this, particle reduction method have been widely adopted, simplifying complex multi-degree-of-freedom (MDOF) system into MDOF systems with reduced degrees of freedom. These reduced-order models retain the essential dynamic properties and critical parameters of the structure, enabling efficient analysis without significant loss of accuracy. This approach has proven valuable in various applications, including wind-induced response prediction, control strategy optimization, and structural health monitoring. This paper focuses on the principles of mass reduction modeling and its application in wind response analysis of high-rise buildings, aiming to provide a practical and reliable framework for evaluating and optimizing wind resistance in tall structures.

2. 60-DOF model

2.1 Frame model

In this study, a building with height H_f = 240 m, depth D_f = 64 m, breadth B_f = 40 m, and side length ratio D_f/B_f of = 1.6 is taken as the object. The layer height of the model is h_i = 4 m, then the number of particles N of the model is N = 240/4 =60. The average density of the frame is ρ_f = 200 kg/m^3. The natural period T_f of the structure is: $T_f = 0.02H_f = 4.8$ s. The mass m_i of a particle i is calculated according to Eq. (1). The frame stiffness k_i of the i floor is determined according to Eq. (2)[1].

$$m_i = \frac{\rho_f \cdot A_f \cdot B_f \cdot D_f}{N} \tag{1}$$

$$k_i = \frac{{}_1\omega_f^2 \cdot m_i \cdot {}_1\phi_i + k_{i+1}({}_1\phi_{i+1} - {}_1\phi_i)}{{}_1\phi_i - {}_1\phi_{i-1}} \tag{2}$$

In this study the first natural mode of the building is a straight line(${}_1\phi = [0.016, 0.033 \ldots 1]^{\mathrm{T}}$). Note that, the frame is assumed to be elastic.

2.2 Setting of the Damper `

When using a shear-type model in which the modeled damper is arranged in parallel with the modeled frame spring, the effective deformation acting on the damper tends to be overestimated, leading to conservative evaluations. To address this, similar to reference 2), a series spring stiffness k_{bi} is introduced alongside the damper stiffness k_{di} to mitigate this overestimation. This paper employs a shear-type model that accounts for layer bending deformation (Fig. 4), with the series combination of k_{di} and k_{bi} defined as the additional system stiffness k_{ai}. The effective deformation ratio α_{ei}, which is used in calculating k_{ai}, is assumed to vary linearly between the layers, following reference 3), with values ranging from 1 at the first layer to 0.1 at the Nth layer (Fig. 3). Furthermore, the yield shear force Q_{ayi} of the additional system is equal to Q_{dyi}.

The damper used in this product is modeled as full plasticity and added to the whole layer. α_{dy1} is damper yield shear force coefficient of the first layer. R_{dy} is damper yield deformation angle. The shear force Q_{dyi} of the damper yield layer of each layer is based on the shear force Q_{dy1} of the first damper yield layer as the reference, and is divided into four stages based on the shear force of the seismic layer for design based on Ai distribution(Fig. 2).

The Q_{dy1}, calculated using the following equation:

$$Q_{dy1} = \alpha_{dy1} \cdot W \tag{3}$$

where W : total weight of the structure.

Interlayer deformation δ_{dyi} is

$$\delta_{dyi} = R_{dy} \cdot h_i \tag{4}$$

The damper stiffness k_{di} is obtained by

$$k_{di} = Q_{dyi}/\delta_{dyi} \tag{5}$$

$$k_{ai} = Q_{ayi}/(\delta_{dyi}/\alpha_{ei}) \tag{6}$$

In addition, additional series surrender deformation are represented by the following equation:

$$\delta_{ayi} = \delta_{dyi}/\alpha_{ei} \tag{7}$$

The effective deformation ratio of story i α_{esi} can be calculated using the following equation:

$$\alpha_{esi} = \alpha_{es1} + (\alpha_{esn} - \alpha_{es1}) \cdot \frac{i-1}{N-1} \tag{8}$$

where, α_{esn} is the effective deformation ratio of n^{th} story.

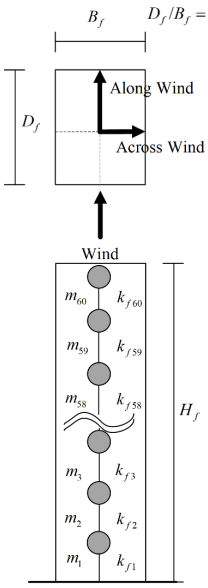

Fig 1. Summary of analytic frame construction

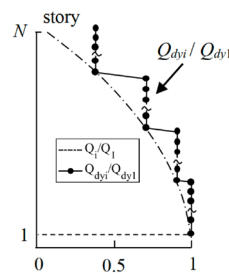

Fig. 2 Yield shear ratio

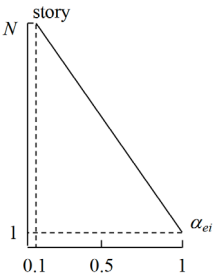

Fig. 3 Effective damper deformation

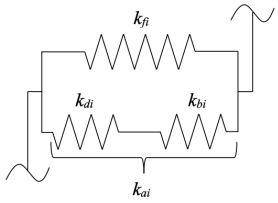

Fig. 4 Frame and damper mode

3. Wind wind force information of the research

The results of CFD[4] (ground surface roughness classification III[5]) were used for wind force. Table 1 and Table 2 list the calculation method of CFD and the calculation conditions. The model used was a prismatic body with a height of 400 mm, a B/D =1.6, and an H/B = 6.0 which are same as target building shown in 2.1 section. The measurements were taken at 60 layers for wind force evaluation.

Table 1. Simulation settings

Algorism	Finite Difference Method (FDM)
Code	Kazamidori® (in-house code)
Fundamental equations	Navier-Stokes equations
Turbulence model	Large Eddy Simulation（LES）
SGS model	Coherent structured Smagorinsky
Spatial difference scheme	2nd order centered difference scheme
Time scheme	3rd order Adams-Bashforth method and Clank-Nicolson method
Poisson solver	Residual cutting method
Grid system	Non-uniform staggered grid system

Table 2. Simulation conditions

Calculation domain	Along-wind direction : 37.5*H* Across-wind direction : 37.5*H* Vertical direction : 5.25*H*
Grid number	About 1.5×10^7
Minimum grid size	0.008*B*
Calculation time	about 10min in full-scale×5waves
Time interval	1.0×10^{-5}s
Inflow boundary	Pre-calculated inflow (Fig.1) U_H=10m/s
Downstream boundary	Convective boundary conditions
Lateral and upper surface boundaries	Zero gradient condition
Ground and building surface boundaries	Wall function (two-layer model)

Fig. 5 shows the wind time history of the top story (story 60) and the PSD of 1st mode generated by CFD compared to the PSD of the AIJ[5]when the wind input is along and across direction.

As shown in the figure, the first-mode wind power spectral density obtained from CFD demonstrates a high level of consistency with the results from AIJ. This indicates that the wind forces generated using the CFD approach in this study are reliable.

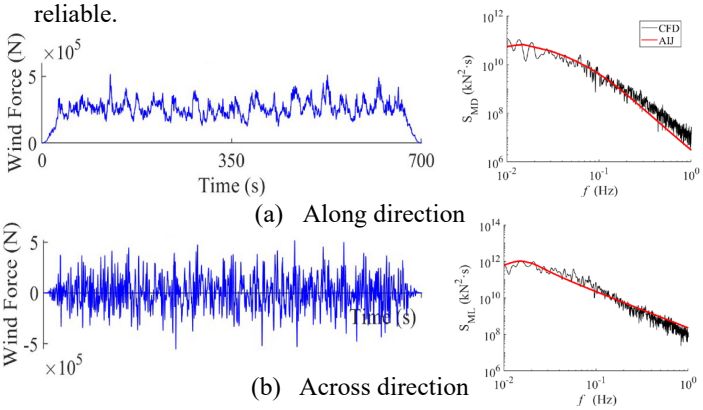

Fig 5. Wind time history of 60th story and PSD of 1st mode

4. Reduction method

4.1 Reduction of the frame model

Fig. 7 shows an outline of the reduction method adopted this time.

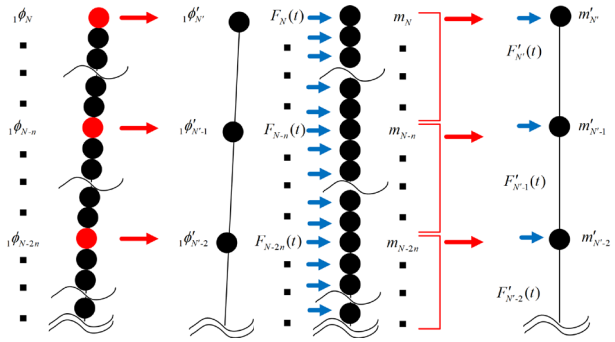

(a) 1st Eigen mode (b) mass and wind load

Fig 7. Outline of reduction

This describes a method for reducing N mass points to N' mass points. The first-order mode vector after the reduction is calculated from:

$$ {}_1\phi'_j = {}_1\phi_{\eta j} \tag{9}$$

using the mass point ratio η ($=N/N'$, η is an integer) and the first-order mode vector before the reduction, assuming that the first-order mode vector after the reduction is equal to the first-order mode vector of the corresponding layer before the reduction.

The mass m'_j after the reduction is expressed as the sum of the reduction layers, and is obtained from Eq. (1) using n and m_i before the reduction.

$$ m'_j = \sum_{i=\eta(j-1)+1}^{\eta\cdot j} m_i \tag{10}$$

The stiffness k'_{fj} after the reduction is expressed by the following equation using the first-order mode vector, mass m'_j after the reduction and the first-order circular frequency.

$$ k'_{fj} = \frac{{}_1\omega_f^2 \cdot m'_j \cdot {}_1\phi'_{fj} + k'_{fj+1}\left({}_1\phi'_{fj+1} - {}_1\phi'_{fj}\right)}{{}_1\phi'_{fj} - {}_1\phi'_{fj-1}} \tag{11}$$

The stiffness of the system k'_j after the reduction is expressed by the following equation:

$$k'_j = \frac{{}_1\omega^2 \cdot m'_j \cdot {}_1\phi'_j + k'_{j+1}\left({}_1\phi'_{j+1} - {}_1\phi'_j\right)}{{}_1\phi'_j - {}_1\phi'_{j-1}} \tag{12}$$

4.2 Reduction of the damper

The stiffness k'_{aj} of the contracted additional system is expressed using the stiffness k'_j of the contracted vibration control model and the stiffness k'_{fj} of the fra after reduction as follows:

$$k'_{aj} = k'_j - k'_{fj} \tag{13}$$

The yield displacement of the additional system after the reduction is obtained by using the method of the yield displacement of the additional system:

$$\delta'_{ayj} = R'_{ayj} \cdot h'_j \tag{14}$$

Here, R'_{ayj}: the interlayer deformation angle of the additional system after the reduction, is assumed to be equal to the yield interlayer angle of the corresponding layer, can be calculated from:

$$R'_{ayj} = R_{aynj} \tag{15}$$

h': the distance between mass points in the model after the reduction, can be calculated from:

$$h'_j = \sum_{i=\eta(j-1)+1}^{n\cdot j} h_i \tag{16}$$

Therefore, the yield shear force Q'_{ayi} of the additional system is calculated as follows:

$$Q'_{ayj} = k'_{ayj} \cdot \delta'_{ayj} \tag{17}$$

4.3 Reduction method of wind forces

The wind forces are also reduced to match the degrees of freedom of the reduced structural model. The method in reference 7) was used to reduce the wind power.

Here, we consider a generalized case where the wind forces of the original model with N degrees of freedom are reduced to wind forces with N' degrees of freedom. We introduce a reduction transformation matrix $[T]$, where T_{nm} represents the element in the nth row and mth column of the $N\times N'$ matrix. If the displacement of the mth layer of the original model corresponds to the displacement of the n th layer of the reduced structure model, $T_{nm} = 1$. If there is no corresponding degree of freedom, we set $T_{kl} = 0$. Using $[T]$, the condition for displacement equivalence can be expressed as follows.

$$\{y'\} = [T]\{y\} \tag{18}$$

Here, $\{y\}$ is the displacement vector of the original model, and $\{y'\}$ is the displacement vector of the reduced structure model. The force-displacement relationships for both models are expressed as follows.

$$\{F\} = [K]\{y\}, \{F^*\} = [K^*]\{y^*\} \tag{19a.b}$$

$[K]$ and $[K^*]$ are the stiffness matrices of the original model and the reduced structure model, respectively, representing the restoring force resistance of each model. From Eqs. (18) and (19.ab), the reduced wind force $\{F^*\}$ is expressed as follows.

$$\{F^*\} = [K^*][T]\{y\} = [K^*][T]\left[K^{-1}\right]\{F\} \tag{20}$$

5. Comparison of results before and after reduction

This chapter compares the dynamic response results of the structure reduced using the novel method proposed in Chapter 4 with those obtained from the structure reduced using existing reduction method[6] for vibration-controlled high-rise buildings, as well as with the dynamic response results of the original structure, to validate the superiority of the proposed method.

5.1 Comparison of results without the damper

This part shows the comparison of the dynamic response results of the model before and after reduction without adding dampers.

Table 3 Natural period without dampers, unit: s

	60DOF	10DOF
1st	4.80	4.80
2nd	1.96	1.96
3rd	1.24	1.24

Fig. 8 shows the first three mode before adding the damper.

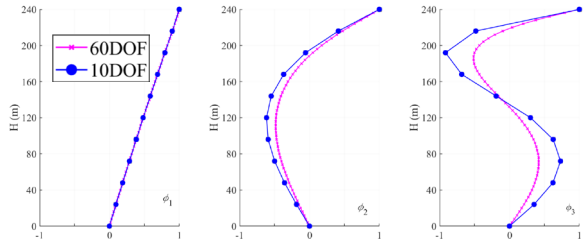

(a) 1st. (b) 2nd (c) 3rd

Fig 8. Mode shape without dampers

Fig. 9 shows the comparison of the dynamic response results of the model before and after reduction without adding dampers. Including the structure's interlayer displacement angle, acceleration. It can be seen from the figure that the dynamic response results of the reduced structure using the new method are more consistent with those of the original structure.

5.2 Comparison of results with the damper

In this case, The damper yield shear force coefficient α_{dy1} of the first layer is 0.005. Damper yield deformation angle Rdy is 1/1000. The $\alpha_{es1} = 1$, $\alpha_{es60} = 0.1$. The relationship from the bottom to the top is linear.

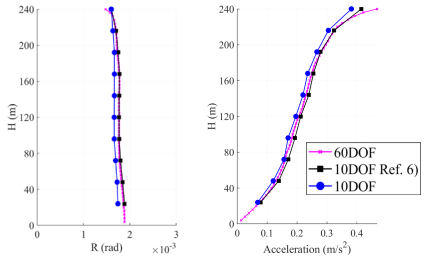

(a) Along

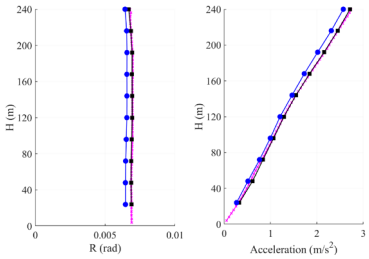

(b) Across

Fig 9. Response without dampers

Table 4. Natural period with dampers, unit: s

	60DOF	10DOF
1st	4.57	4.57
2nd	1.88	1.87
3rd	1.18	1.18

Fig. 10 shows the first three modes of the system.

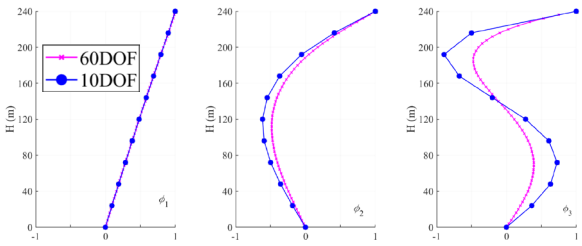

(a) 1st (b) 2nd (3) 3rd

Fig 10. Mode shape with dampers

This part of the picture shows the dynamic response of the structure when the wind input is along and across directions with the addition of dampers. It can be seen from the figure that the dynamic response results of the reduced structure using the new method are more consistent with those of the original structure. From the figure, it can be observed that after adopting the optimized new method, reducing the original structure to a 10- mass-point model significantly improves the accuracy of the dynamic response of the reduced structure.

6. Conclusion

This study introduced a novel reduction method for high-rise building damper systems and evaluated its effectiveness

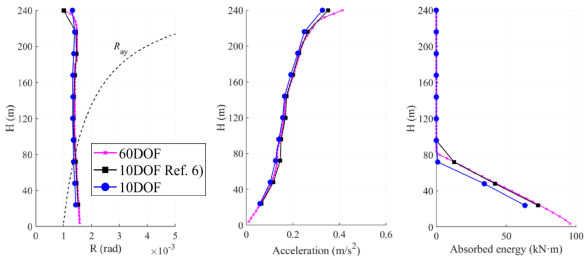

(a) Along

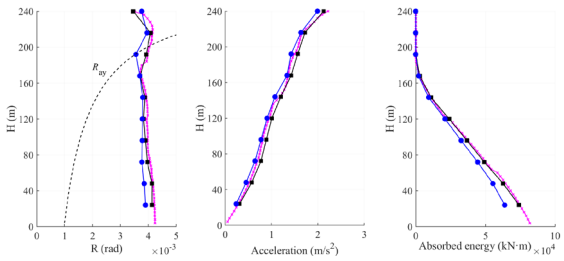

(b) Across

Fig 11. Response with dampers

through dynamic response analyses. By simplifying the original 60-degree-of-freedom (DOF) model to a 10-DOF model, the proposed approach was shown to maintain high accuracy in critical response parameters such as displacement, velocity, and acceleration under wind load conditions. Furthermore, the results demonstrated that the new reduction method offers improved precision in interlayer drift and absorbed energy compared to previous methods.

The study highlighted the importance of preserving essential structural dynamics while achieving computational efficiency. The introduction of displacement equivalence for wind force reduction ensured that wind load effects were accurately captured in the reduced model. This advancement not only reduces computational demand but also provides a reliable tool for analyzing wind-induced structural behavior in high-rise buildings.

Future work could expand the application of this method to nonlinear systems or investigate its efficacy under combined wind and seismic loads.

Reference

1) Daiki Sato, Kazuhiko Kasai and Tetsuro Tamura, Influence of Frequency Sensitivity Of Viscoelastic Damper, J.Struct. Constr. Eng., AIJ, Vol.74 No.635, 75-82,Jan. 2009
2) Tsuji Masaaki, Kokubu Hiroki, Yoshitomi Shinta, Takewaki Izuru, Optimal Placement Method Using a Reduced Structural Model for Vibration Control Dampers with Nonlinear Restoring Force Characteristics, Transactions of AIJ: Journal of Architecture and Building Science, Vol. 75.
3) Masato Ishii and Kazuhiko Kasai： Shear Spring Model For Time History Analysisof Multistory Passive Controlled Buildings，J.Struct. Constr. Eng,Aij,Vol.75 No.647，103-112,Jan. 2010
4) OKIMURA Masahiro, SATO Daiki, TANAKA Hideyuki, SONE Takayuki,WATAl Kazuki, AZEGAMl Yasuhiko, KONNO Daisuke, Index for evaluating the impact of wind force on the response of high-rise buildings Part2 Methods of constructing evaluation indicators andits validation, J.Struct. Constr. Eng.,AIJ,pp. 469-472, 3,2024
5) AIJ Recommendations for Loads on Buildings (2015)
6) Chihiro Suzuki, Masaaki Tsul, Shinta Yoshitomi and Lzuru Takewaki, Reduced Load And Structure Models Via Inverse Formulation For Time-History Wind Response Analysis Of High-Rise Buildings, J.Struct. Constr. Eng.,AIJ,Vol.74 No.640, 1073-1081, Jun.,2009
7) Koki Hiratsuka, Daiki Sato, Hideyuki Tanaka, Prediction method of damper yield and cumulative damage distribution of high-rise building with hysteretic damper Part.1 Verification of reduced model, J.Struct. Constr. Eng.,AIJ,pp. 501-504, 3,2020

*1 Institute of Science Tokyo

*2 Takenaka Corporation